

PH DEPENDENT CONFORMATIONAL DYNAMICS OF SUBSTITUTED
TRIAZINES

by

NICHOLAS CHARLES HENDERSON

Bachelor of Science, 2019

Texas Christian University

Fort Worth, Texas

Submitted to the Graduate Faculty of the

College of Science and Engineering

Texas Christian University

in partial fulfillment of the requirements

for the degree of

Master of Science

May 2022

PH DEPENDENT CONFORMATIONAL DYNAMICS OF SUBSTITUTED
TRIAZINES

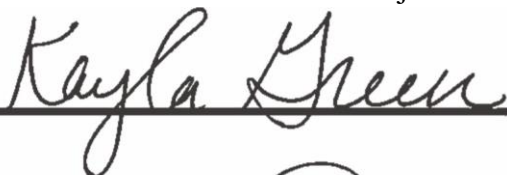
by

Nicholas Charles Henderson

Thesis approved:



Major Professor







For the College of Science and Engineering

ACKNOWLEDGEMENTS

I would like to thank Dr. Janesko for his patience and guidance over the years. His dedication to his work and willingness to work with me is what has made this project and degree possible. I would also like to thank Dr. Green, Dr. Simanek, Dr. Minter, and Dr. Conrad for all their support and encouragement throughout the last two and a half years. It is individuals like them who make the TCU chemistry department an incredible place to learn and work.

TABLE OF CONTENTS

Acknowledgements.....	ii
List of Figures.....	iv
List of Tables.....	v
1. Introduction.....	1
2. Computational Methods.....	4
2.1 Gaussian calculation setup.....	4
2.2 Validating DFT predictions of triazine pK_a and protonation sites.....	5
2.3 Validating DFT predictions of NRR' rotational barriers in substituted aminotriazines.....	5
2.4 Testing hypotheses 1 and 2, that protonation changes the rotational barriers of substituted aminotriazines	6
2.5 Predicting pK_a values.....	8
3. Results	11
3.1 Validation of DFT-predicted triazine pK_a	11
3.2 Validation of hypothesis 3, ring protonation is preferred over acyclic protonation..	13
3.3 Validation of the computed geometries and C-N bond order of 2-amino-1,3,5- triazine.....	14
3.4 Computed rotational barrier of acyclic groups in neutral aminotriazines.....	17
3.5 Ring protonation increases rotational barriers of amino groups on substituted triazines by 3-5 kcal/mol.....	19
3.6 A test of hypothesis number 2, that protonation at the NRR' acyclic amino group nitrogens decrease rotational barriers.....	22
3.7 Acyclic protonation barrier results provide further support that triazines become conformationally flexible at high pH.....	23
4. Discussion.....	28
4.1 Rotational barrier discussion.....	28
4.2 pK_a discussion.....	30
5. Conclusion.....	30
References.....	32

Vita

Abstract

LIST OF FIGURES

1.1. Depicts 2,4,6-tri(amino)-1,3,5-triazine (melamine) on the top, and a generic triazine on the bottom. Both structures are important to this study.....	1
1.2. Depicts the triazine of interest presented by the Simanek group, the arrows indicate the rotation about the acyclic nitrogen and the ring carbon. This results in four possible rotational isomers.....	3
1.3. Resonance structures of neutral, ring protonated, and acyclic protonated form of the generic triazine. 2b supports hypothesis 1, that protonation on the ring increases the rotational barrier of the acyclic amino group. 2c shows a tetrahedral amino nitrogen, supporting hypothesis 2. It is believed that 2b is preferred over 2c.	3
2.1. Depicts the rotational scheme used to calculate the rotational barriers, where R=Me, H.....	2
2.2. Depicts how the second angle in the dihedral is changed at 60 degrees to find the lowest energy conformation in the rotational barrier.....	8
2.3. Depicts the proton transfer from a melamine derivative to melamine, in this example, the proton transfer from 2,4-diamino-6-dimethylamino-1,3,5-triazine to melamine is depicted. The Gibbs free energy of this proton transfer was used to determine the pK_a	9
2.4. Depicts the 10 structures (in their most stable conformations) used to compute pK_a	10
3.1. A graph of the DFT computed pK_a values for melamine derivatives compared to experimental pK_a values for melamine derivatives.....	12
3.2. Optimized structures of the 2-amino-1,3,5-triazine molecules obtained from gaussian output files.....	16
3.3. The one-dimensional potential energy scan of 2-methylamino-1,3,5-triazine.....	18
3.4. The one-dimensional potential energy scan of 2-dimethylamino-1,3,5-triazine.....	19
3.5. The one-dimensional potential energy scan of 2-amino-1,3,5-triazine in its ortho protonated form.....	20
3.6. The one-dimensional potential energy scan of 2-methylamino-1,3,5-triazine in its ortho protonated form.....	21
3.7. The one-dimensional potential energy scan of 2-dimethylamino-1,3,5-triazine in its ortho protonated form.....	22
3.8. The one-dimensional potential energy scan of 2-amino-1,3,5-triazine in its acyclic protonated form.....	24
3.9. The one-dimensional potential energy scan of 2-methylamino-1,3,5-triazine in its acyclic protonated form.....	25
3.10. The one-dimensional potential energy scan of 2-dimethylamino-1,3,5-triazine in its acyclic protonated form.....	26

3.11. The one-dimensional potential energy scan of 2-amino-1,3,5-triazine in blue, compared to the one-dimensional potential energy scan of 2-dimethylamino-1,3,5-triazine in orange..... 27

LIST OF TABLES

3.1. DFT computed pK_a values and their error compared to experiment for ring protonated species.....	13
3.2. DFT computed pK_a values for the acyclic protonated species compared to experimental pK_a s (where the protonation occurs on the ring).....	14
3.3. Computed bond lengths (in Å) for C-N bonds in 5 different compounds.....	16
3.4. This figure shows the pyramidalization angle of 2-amino-1,3,5-triazine at different dihedral angles	18
3.5. Computed rotational barriers and pK_a values for 2-amino-1,3,5-triazine, 2-methylamino-1,3,5-triazine, and 2-dimethylamino-1,3,5-triazine.....	28

1. Introduction

Triazines (fig 1.1) are a class of molecule that serves an important purpose for industrial chemists. Triazines are often used as building blocks for dendrimers and macrocycles which are of high interest to the pharmaceutical industry mainly for their use in therapeutics and drug delivery.^{1,2} Abbasi, et al. define dendrimers as “nano-sized, radially symmetric molecules with well-defined, homogeneous, and monodisperse structure that has a typically symmetric core, an inner shell, and an outer shell”.³ Yudin defines a macrocycle as “a molecule that contains a cyclic framework of at least twelve atoms”,⁴ both types of molecules can be synthesized using triazines as building blocks. Dendrimers and macrocycles can consist of multiple triazines and hundreds of atoms.

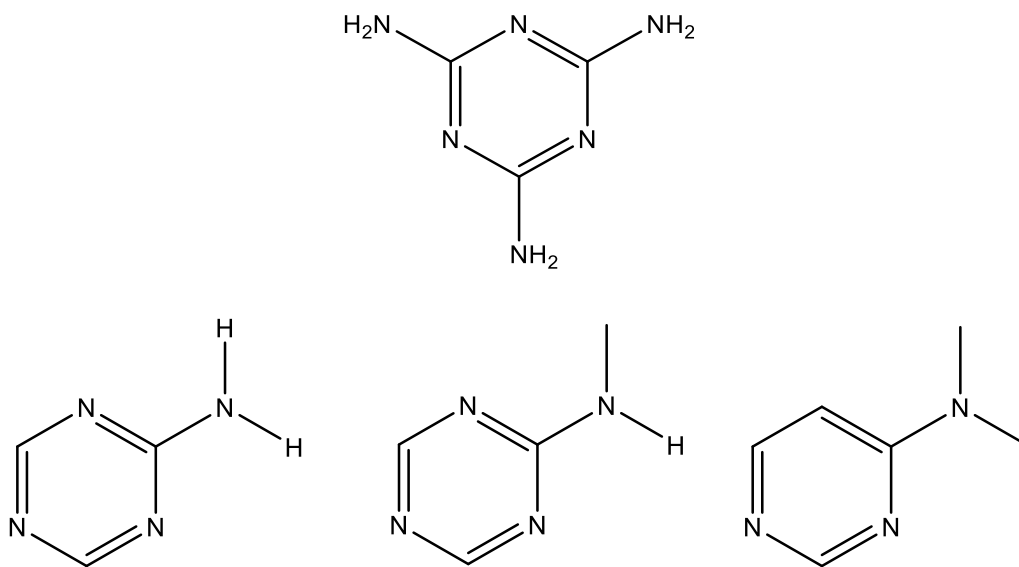


Figure 1.1 Depicts 2,4,6-tri(amino)-1,3,5-triazine (melamine) on the top, and a generic triazine on the bottom. Both structures are important to this study.

Tri(amino)triazine dendrimers exhibit many remarkable properties. Examples include acting as antibacterial agents⁵ and platelet activation⁶. Large triazine structures even show potential as

anti-tumor drugs. These molecules exhibit host-guest binding properties under physiological conditions by binding to tumor cells.⁵ Macrocycles containing tri(amino)triazines show potential for use in therapeutics² and drug delivery systems including certain chemotherapy drugs.⁷

Triazines can be protonated in aqueous solution under acidic conditions. Protonation is expected to affect the rotational barrier and conformation dynamics of triazines. NMR data in a study of macrocycles by the Simanek group indicates that upon protonation in the ortho position on an aminotriazine (figure 1.2), the rotation of the amino group either increases or decreases in speed.² Resonance structures of generic aminotriazines support this theory by illustrating that protonation changes the double bond character between the ring carbon and the amino group nitrogen (figure 1.2). This has led to four hypotheses. 1, protonation at the ring nitrogen increases rotational barrier of the acyclic amino group. 2, protonation at the acyclic amino group nitrogen decreases rotational barriers. 3, for most R groups, aminotriazines will be protonated at the ring nitrogen at modest pH and will protonate the acyclic amino group nitrogen at low pH (extremely acidic conditions). 4, aminotriazine based molecules will tend to rigidify at moderate pH ~4-5 due to ring nitrogen protonation, then become conformationally flexible again at low pH ~1-2 due to acyclic amino nitrogen protonation.

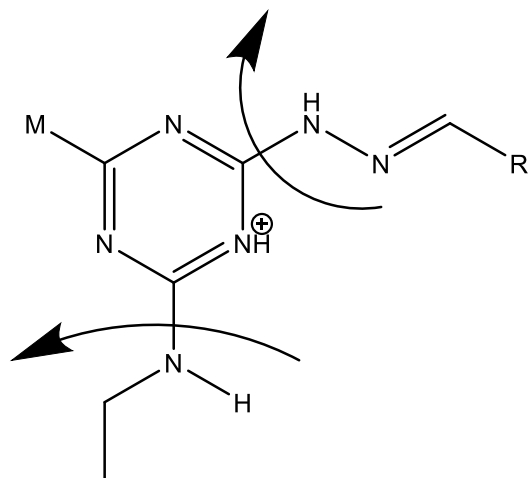
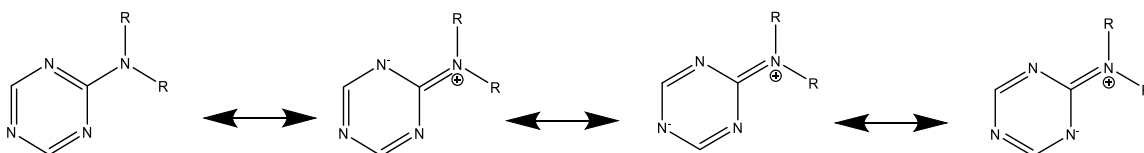
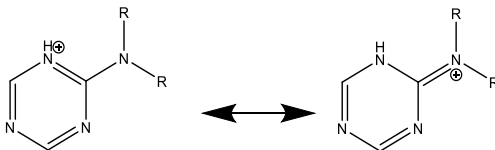


Figure 1.2 Depicts the triazine of interest presented by the Simanek group, where M is morpholine. The arrows indicate the rotation about the acyclic nitrogen and the ring carbon. This results in four possible rotational isomers.

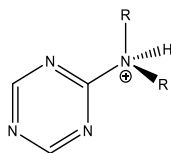
Our plan is to perform an in-depth study of triazine dynamics in aqueous solution using modern Density Functional Theory (DFT).⁸ The goal is to simulate dynamics of triazines, with the plan to test if our initial expectations in hypothesis 1-4 are consistent with the predicted results. The hope is that this may provide useful tools for both experimentalists and computational chemists to model the behaviors of systems like dendrimers and macrocycles.



1.3a. Resonance structures of the generic triazine in its neutral form (R=Me, H).



1.3b. Resonance structures of the generic triazine in its ortho protonated form (R=Me, H).



1.3c. Resonance structures of the generic triazine in its acyclic protonated form (R=Me, H).

Fig 1.3 shows resonance structures of neutral, ring protonated, and acyclic protonated form of the generic triazine. 2b supports hypothesis 1, that protonation on the ring increases the rotational barrier of the acyclic amino group. 2c shows a tetrahedral amino nitrogen, supporting hypothesis 2. It is believed that 2b is preferred over 2c.

2. Computational methods

2.1 Gaussian calculation setup

All calculations were performed using the Gaussian 16 electronic structure package.⁹ Gaussview 6 was used to prepare input files and examine output files.¹⁰ Rotational barrier calculations of substituted aminotriazines in acyclic protonated, ring protonated, and neutral form were all performed. pK_a calculations utilized a literature test set of melamine derivatives.¹¹ Computations used the density functional theory (DFT)⁸ at the M062X/6-311++(2d,2p)^{12,13} level using the solvent model based on density (SMD) in continuum water.¹⁴ Geometry optimizations were performed in the same SMD continuum solvent water as well.

The 6-311++(2d,2p) basis set¹³ choice is consistent with other calculations on similar nitrogen containing aromatic structures.¹⁵ Due to the water-soluble nature of melamine

derivatives¹⁰, a continuum solvent water model was chosen to model their nature in water. A computational study by Galvez et al. studied rotational barriers of 2-aminopyridine, 2-aminopyrimidine, and N-methylamino-1,3,5-triazine and used the 6-311++(2d,2p) basis set for all rotational barrier calculations.¹⁵

2.2 Validating DFT predictions of triazine pK_a and protonation sites

Predicting pK_a values by DFT methods required checks to confirm DFT calculations were consistent with general knowledge of organic chemistry. Melamine derivatives show double bond character between the ring carbon and the amino nitrogen. To test if the DFT calculations show consistency with resonance structure predictions, analysis of output files needed to be performed. Computed data should indicate increased double bond character between the ring carbon and the acyclic nitrogen for neutral and ring protonated species and should lack double bond character for the acyclic protonated species.

Once it was confirmed that DFT methods were consistent with experiment, DFT pK_a calculations were considered reliable. Further validation of the DFT methods could be later enforced by showing consistency between computed pK_a values and experimental pK_a values for melamine¹⁶ and melamine derivatives.¹¹

2.3 Validating DFT predictions of NRR' rotational barriers in substituted aminotriazines

To confirm DFT calculations are 1, consistent with general knowledge of organic chemistry, and 2, produce sensible results, three types of calculations must be performed: acyclic protonation, ortho ring protonated, and neutral species rotational barriers of the acyclic amino group. Even though it is known that initial protonation occurs on the ring to form a 1+ species,^{11,16} and acyclic protonation does not occur except for ultra-acidic, high pH conditions

where a 2+ charge is present (in fact the pK_b of the amino group in melamine would be 17.8),¹⁶ our second hypothesis, that protonation on the acyclic amino group decreases its rotational barrier had to be tested in order to move forward with the study.

2.4 Testing hypotheses 1 and 2, that protonation changes the rotational barriers of substituted aminotriazines

Testing Hypotheses 1 and 2, that protonation changes the rotational barrier of the acyclic amino group requires computing the rotational barriers of neutral, ring protonated, and acyclic protonated aminotriazines. Rotational barrier calculations were performed on three different substituted triazines: 2-amino-1,3,5-triazine ($R_1=R_2=H$), 2-methylamino-1,3,5-triazine ($R_1=Me$, $R_2=H$), and 2-dimethylamino-1,3,5-triazine ($R_1=R_2=Me$), which are illustrated in figure 2.1.

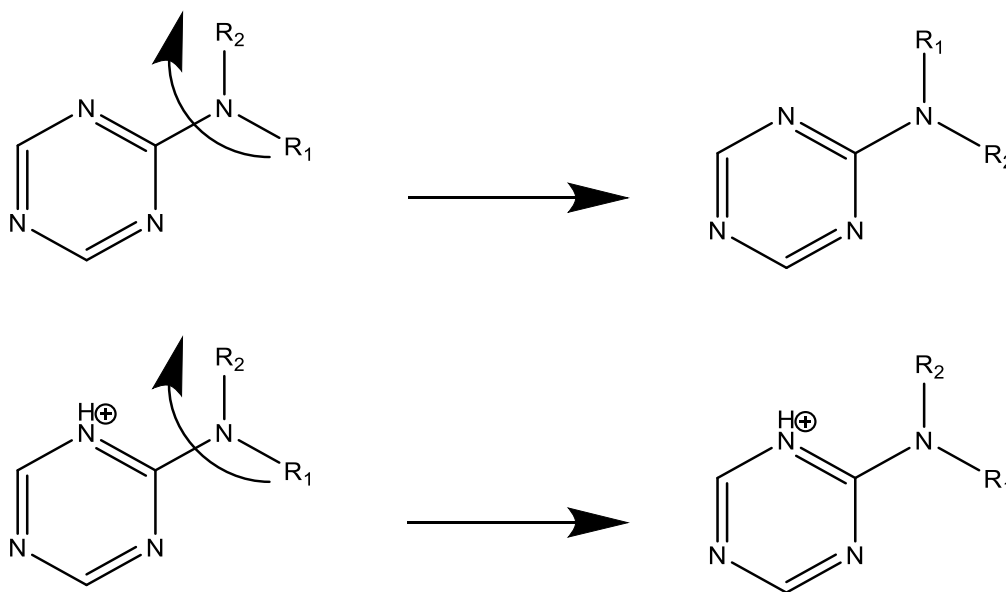


Figure 2.1 Depicts the rotational scheme used to calculate the rotational barriers, where R=Me, H.

Rotational barriers followed the scheme presented in figure 3 and the initial setup of calculations followed the method employed by Galvez et al.¹⁵ The redundant coordinate editor in gaussview¹⁰ was used to set up a relaxed scan of 36 steps at 10-degree intervals. Initial calculations resulted in discontinuities depicted by the blue curve in figure 2.2. Discontinuities are consistent with the initial results produce by Galvez, et al.¹⁵

Rotational barriers of the amino group in triazines involved the rotation of R groups in relation to the aromatic triazine structures. This is depicted by the graph in figure 2.2. The two curves are scans of each of the circled hydrogens dihedral 1-D potential energy surface (PES). Each start at two different geometries, where the initial angle of each circled hydrogen was 60 degrees. The ground state potential energy surface is the lower energy values for both the orange and the blue curve. Conceptually, the idea is that in its lowest energy state, the NRR' group is sp^2 hybridized and nearly planar, but when the dihedral angle is $0^\circ < \Theta < 180^\circ$, the amino group is sp^3 hybridized.

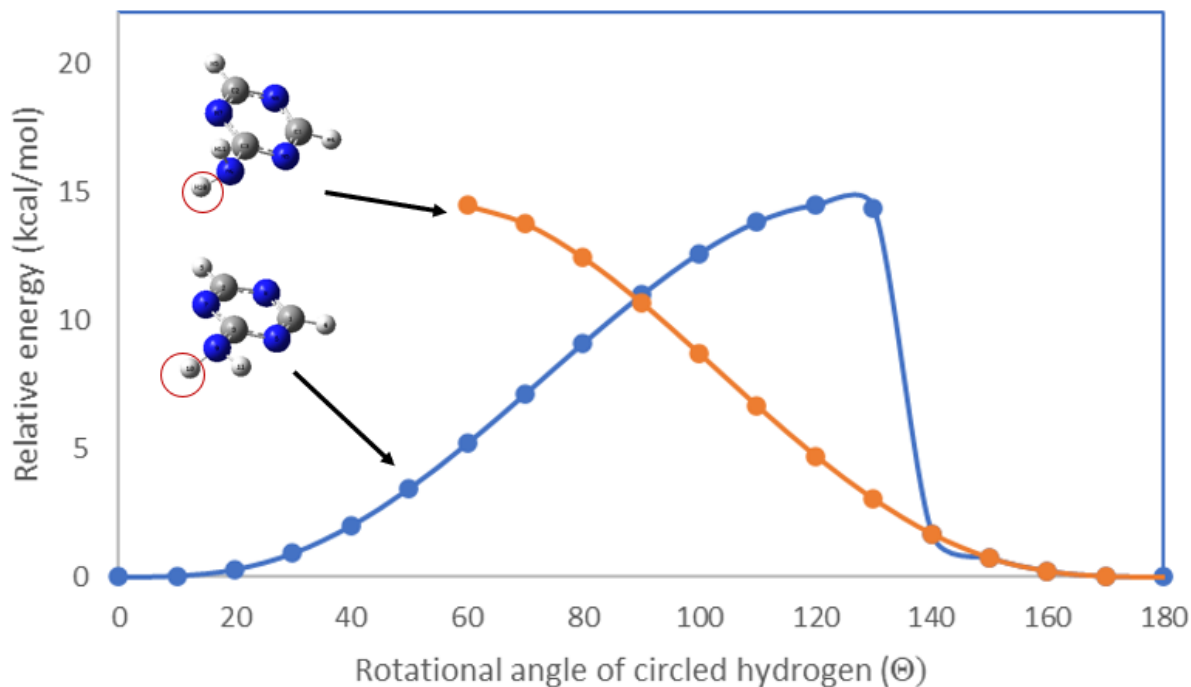


Figure 2.2 Depicts how the second angle is changed when the dihedral angle of the circled hydrogen is 60 degrees, in order to find the lowest energy conformation in the rotational barrier.

2.5 Predicting pK_a values

The goal was to predict the pK_a values of a melamine derivative using DFT calculations.

Literature work by Zeng, et al. indicated that the M06-2X density functional reduces error in pK_a calculations.¹⁷ Several steps had to be employed to carry out this task.

This portion of the study relied on the set of experimentally determined pK_a values of melamine derivatives previously mentioned,¹¹ where the the computed pK_a is a thermodynamic quantity of the proton transfer shown in figure 2.3. Thermodynamic quantites could be taken directly from the log files. ΔG could be found using equation 2.1, where “triazine” represents a melamine derivative,¹¹ and the pK_a relative to melamine was converted from ΔG using equation 2.2.¹⁸

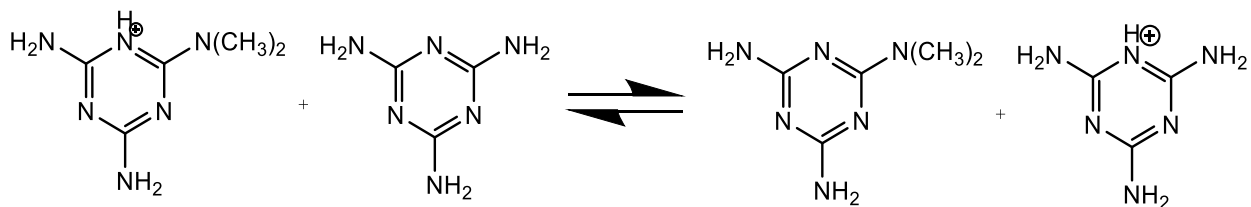


Figure 2.3 Shows the proton transfer from a melamine derivative to melamine, in this example, the proton transfer from 2,4-diamino-6-dimethylamino-1,3,5-triazine to melamine is depicted. The Gibbs free energy of this proton transfer was used to determine the pK_a .

$$\Delta G = (G_{\text{melamine-H}^+} + G_{\text{triazine}}) - (G_{\text{triazine-H}^+} + G_{\text{melamine}}) \text{ eq2.1}$$

$$\text{Computed } pK_a = pK_a(\text{melamine}) + \Delta G / (2.303RT) \text{ eq2.2}$$

Initial calculations required testing every possible conformation of the melamine derivatives from the test set.¹¹ Every possible conformation was tested by running an optimization+frequency calculation in gaussian.⁸ The lowest energy conformation was used to compute pK_a .

Literature sources indicate that protonation occurs on the ring in melamine and its derivatives.^{11,16} Therefore, the next step was to test all possible ring protonation sites on each of the computationally determined most stable conformations. Once the lowest energy protonation site was determined, the pK_a could finally be determined. Figure 2.4 shows the ten different molecules from which their experimental pK_a is used to validate DFT methods, table 1 shows the experimental and computed DFT pK_a values.

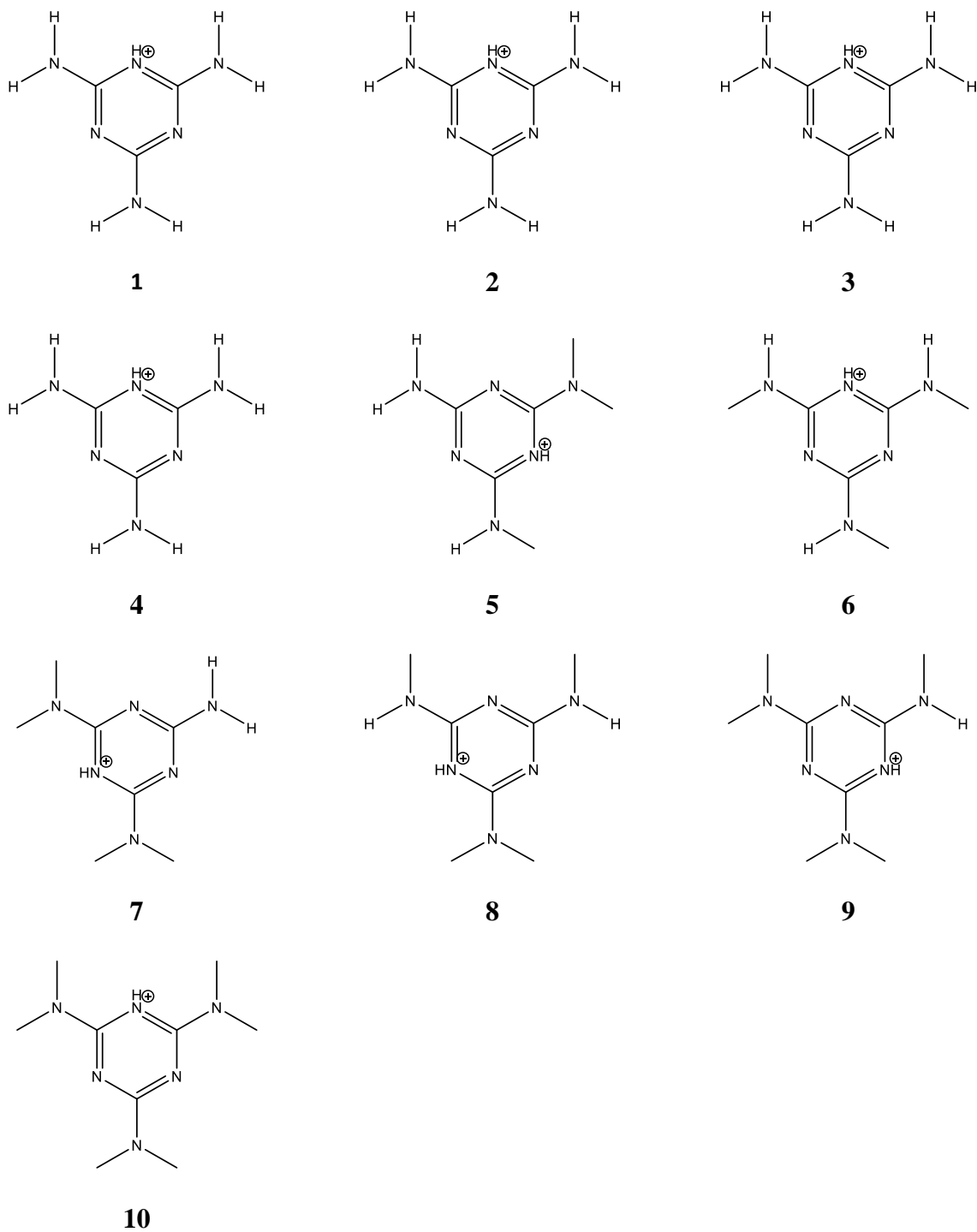


Figure 2.4 Shows the 10 structures (in their most stable conformation) used to compute pK_a .

The initial approach used the standard rigid rotor harmonic oscillator model, which computes ΔS for the translation, vibrational, and rotational motion for every single molecule. This was

employed first due to its straightforward nature, in this case, the ΔG values were taken directly from the gaussian output files and used to compute the pK_a of each melamine derivative. The second approach used constant ΔS and $\Delta G = \Delta H - T\Delta S$. Here, the entropy contribution is treated as $\Delta S = 0$. Computing ΔG in continuum solvent requires the use of a thermodynamic cycle,¹⁹ which requires adding solvent corrections to computed gas phase free energies which can often result in significant error in the entropy term. Neglecting the entropy term results in less error in the calculated ΔG than including the entropy effects from solvent corrections.

3. Results

3.1 Validation of DFT-predicted triazine pK_a

Figure 3.1 depicts a plot of the initial DFT computed pK_a values for nine different melamine derivatives. The R^2 value of ~ 0.9 indicates a good linear correlation between the computed pK_a values and the experimental data.

Furthermore, error analysis shows striking differences in the data. Data produced using the standard rigid rotor harmonic oscillator approximation, which includes solvent corrected entropy terms resulted in a maximum error of 20.4 % and an average error of 11.5 %. Data derived from using constant entropy resulted in a maximum error of 16.1 % and an average error of 9.3 %.

Table 3.1 shows all computed pK_a values that used constant ΔS .

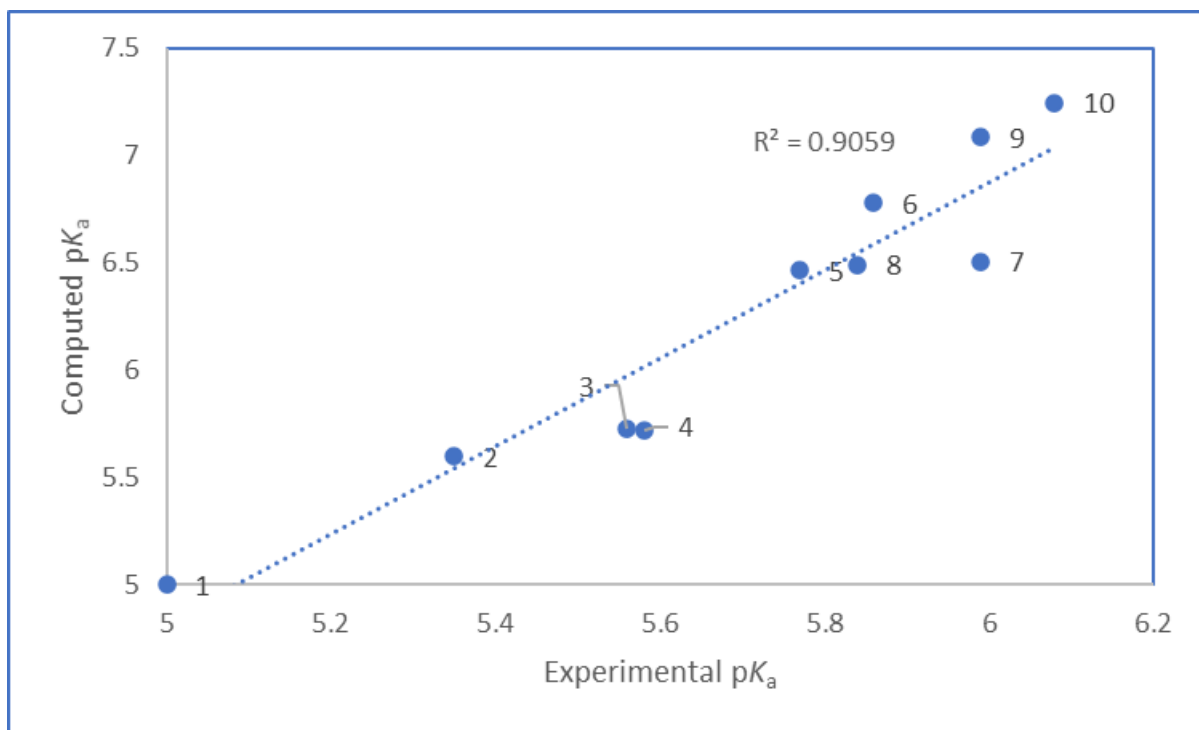


Figure 3.1 Shows the resulting computed pK_a values with the final computational protocols.

Structure (from fig 4)	Computed pK_a	Experimental pK_a	Percent Error
2	5.60	5.35	4.5
3	5.73	5.56	2.9
4	5.72	5.58	2.5
5	6.46	5.77	10.7
6	6.78	5.86	13.6
7	6.50	5.99	8.0
8	6.69	5.84	10.0
9	7.08	5.99	15.4
10	7.25	6.08	16.1

Table 3.1 Shows computed pK_a values and their error compared to experiment for ring protonated species.

3.2 Validation of hypothesis 3, ring protonation is preferred over acyclic protonation

Table 3.2 shows the DFT computed pK_a for the acyclic protonation using equation 2.2. It is evident by the negative pK_a values that acyclic protonation results in a much more acidic hydrogen than a ring protonated triazine. This is further support of the hypothesis that ring protonation is preferred over over acyclic protonation. This data also agrees with experiment.^{11,16}

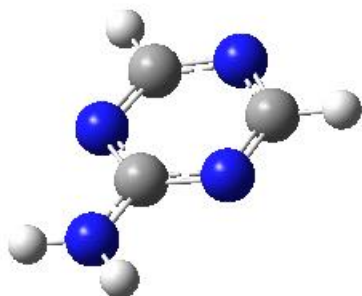
Structure (from fig 4)	Computed pK_a	Experimental pK_a
2	1.32	5.35
3	0.92	5.56
4	1.59	5.58
5	2.37	5.77
6	3.00	5.86
7	3.04	5.99
8	1.49	5.84
9	2.88	5.99
10	5.54	6.08

Table 3.2 DFT computed pK_a values for the acyclic protonated species compared to experimental pK_a values (where the protonation occurs on the ring).

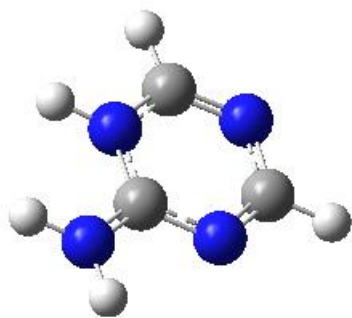
3.3 Validation of the computed geometries and C-N bond order of 2-amino-1,3,5-triazine

Resonance structures indicate that both the ring protonated form and the neutral form of substituted triazines have double bond character between the amino nitrogen and the ring carbon. The acyclic protonated form is tetrahedral. Both of these statements are supported by resonance structures in figure 1, this claim is further supported by data in table 3.3 which shows C-N bond lengths. The experimentally determined bonds lengths for methylamine and methylimine are 1.48 and 1.27 Å respectively.^{20,21} The computed bond lengths for each of the two species are 1.47 and 1.27 Å. The trend observed in computed bond length for neutral, ring protonated, and acyclic 2-amino-1,3,5-triazine that are shown in figure 3.2 is consistent with experimentally observed data for methylamine and methylimine, where double bond character decreases the bond

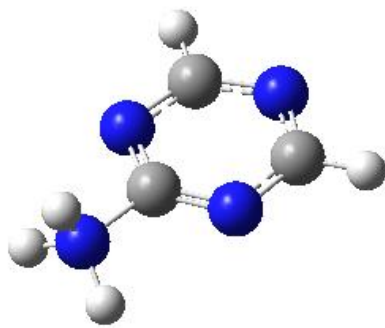
length. Furthermore, the ring protonated species shows a shorter computed bond length than the neutral form, suggesting that it has more double bond character. This is further support of the first hypothesis, that protonation on the ring nitrogen increases the acyclic amino groups rotational barrier.



3.2a. An optimized structure of 2-amino-1,3,5-triazine obtained from the gaussian output file (bond length 1.33 Å) .



3.2b. An optimized structure of 2-amino-1,3,5-triazine in its ortho protonated form obtained from the gaussian output file (bond length 1.31 Å).



3.2c. An optimized structure of 2-amino-1,3,5-triazine in its acyclic protonated form obtained from the gaussian output file (bond length 1.46 Å).

Figure 3.2 Shows optimized structures of the 2-amino-1,3,5-triazine molecules obtained from gaussian output files.

Molecule					
Computed C-N bond length (Å)	1.33	1.46	1.31	1.47	1.27

Table 3.3 Shows computed bond lengths (in Å) for C-N bonds in 5 different molecules.

Previously a concept was introduced suggesting that the hybridization of the amino group changes from sp^2 to sp^3 as the amino group rotates about the C-N bond for a dihedral angle between 0° and 180° . This can be validated by computing the pyramidalization angles of the amino group in 2-amino-1,3,5-triazine and comparing them to the pyramidalization angles in ammonia (sp^3 nitrogen) and ring protonated 4-aminopyridine (sp^2 nitrogen), which are 39.8° and

0° respectively. The values for the computed pyramidalization angles in 2-amino-1,3,5-triazine are shown below in table 3.4. For the purposes of consistency, all calculations were performed at the same M062x/6-311++(2d,2p)^{12,13} level using the SMD continuum water.¹⁴ The results indicate that the acyclic amino group shows sp² character at a dihedral angle of 0° and sp³ character when 0° < Θ < 180°.

Dihedral Angle	Pyramidalization Angle
0°	0°
60°	36.6°
90°	43.0°

Table 3.4 Shows the pyramidalization angle of 2-amino-1,3,5-triazine at different dihedral angles.

3.4 Computed rotational barrier of acyclic groups in neutral aminotriazines

Initial results of neutral species were used to compare the dynamics of ring protonated species to the dynamics of neutral species in solution. Potential energy scans were used to predict the rotational barrier of the acyclic NRR' group attached to the neutral triazine in solution. Figure 3.3 and 3.4 depict the ground state potential energy scans (PES) in terms of relative energy and the rotational angle of the circled atom or group (Θ). The computed rotational barriers for the ground state PES of 2-amino-1,3,5-triazine, 2-methylamino-1,3,5-triazine, and 2-dimethylamino-1,3,5-triazine are shown in table 3.4.

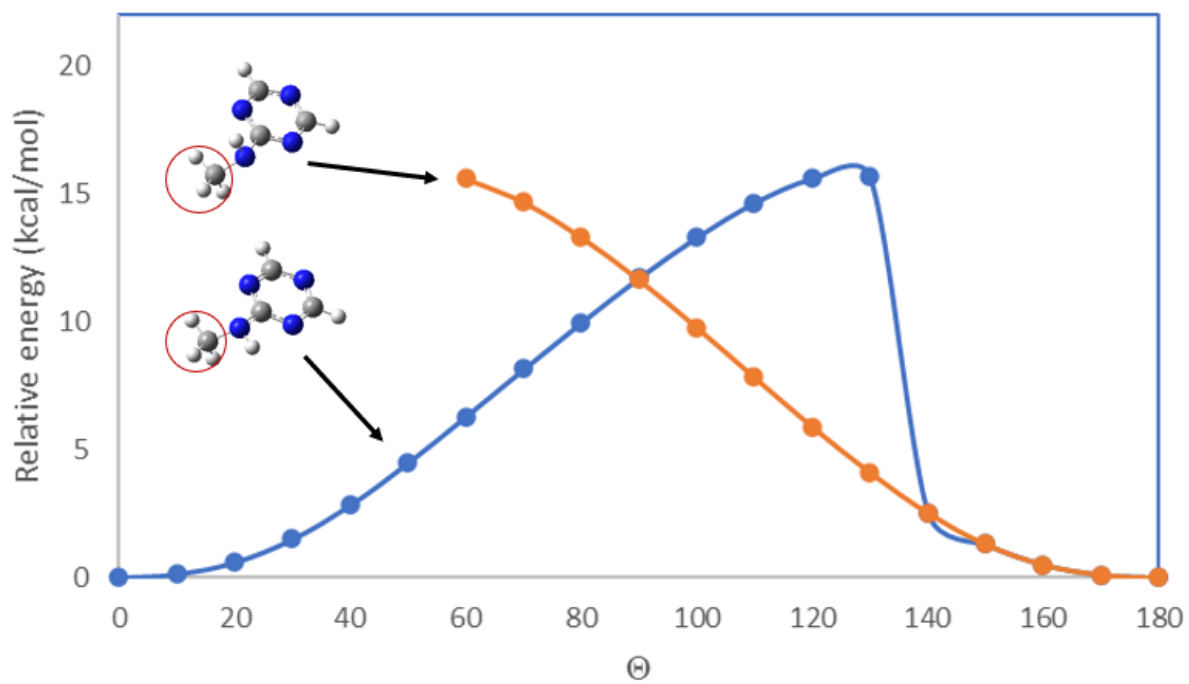


Fig 3.3 Depicts the 1-D potential energy scan of 2-methylamino-1,3,5-triazine.

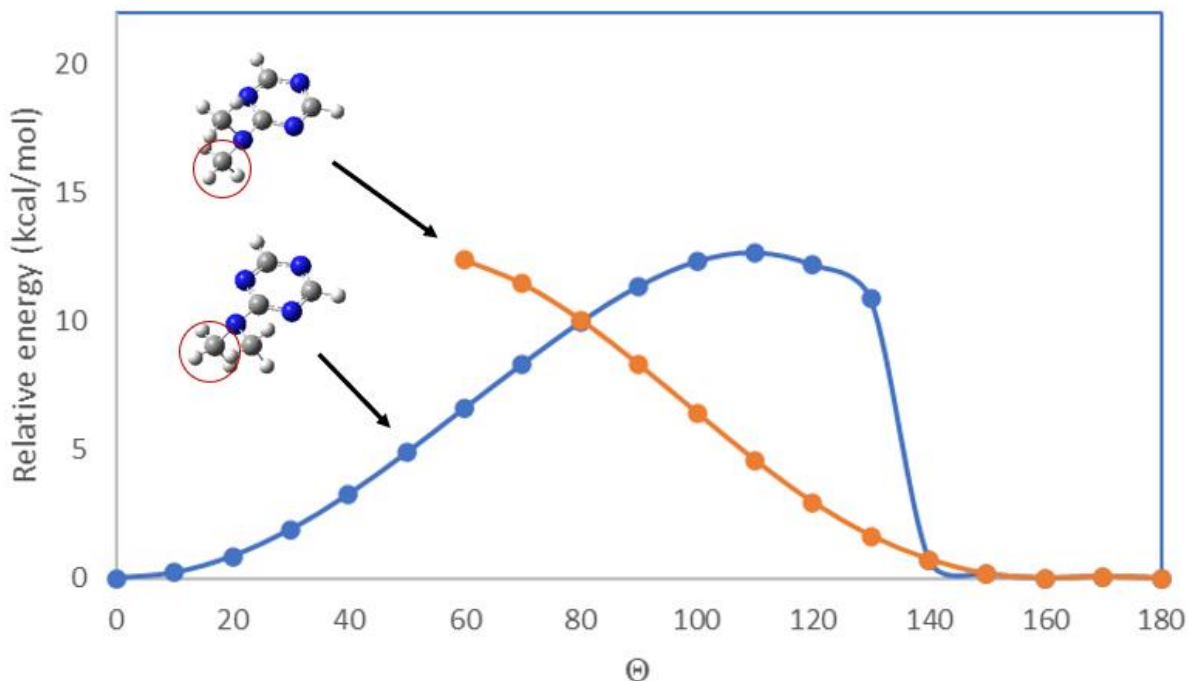


Fig 3.4 Depicts the 1-D potential energy scan of 2-dimethylamino-1,3,5-triazine.

3.5 Ring protonation increases rotational barriers of amino groups on substituted triazines by 3-5 kcal/mol

Hypothesis 1 states that rotational barriers increase when the triazine ring nitrogen is protonated. Figures 3.5, 3.6, and 3.7 show the one-dimensional potential energy scans for ortho protonated 2-amino-1,3,5-triazine, 2-methylamino-1,3,5-triazine, and 2-dimethylamino-1,3,5-triazine structures. The computed rotational barrier of the amino group is increased by 2.36, 4.15, and 5.10 kcal/mol relative to the rotational barrier of the amino group in the neutral species. Table 3.4 shows all computed rotational barriers for the neutral, acyclic protonated, and ring protonated forms of the three substituted triazines studied.

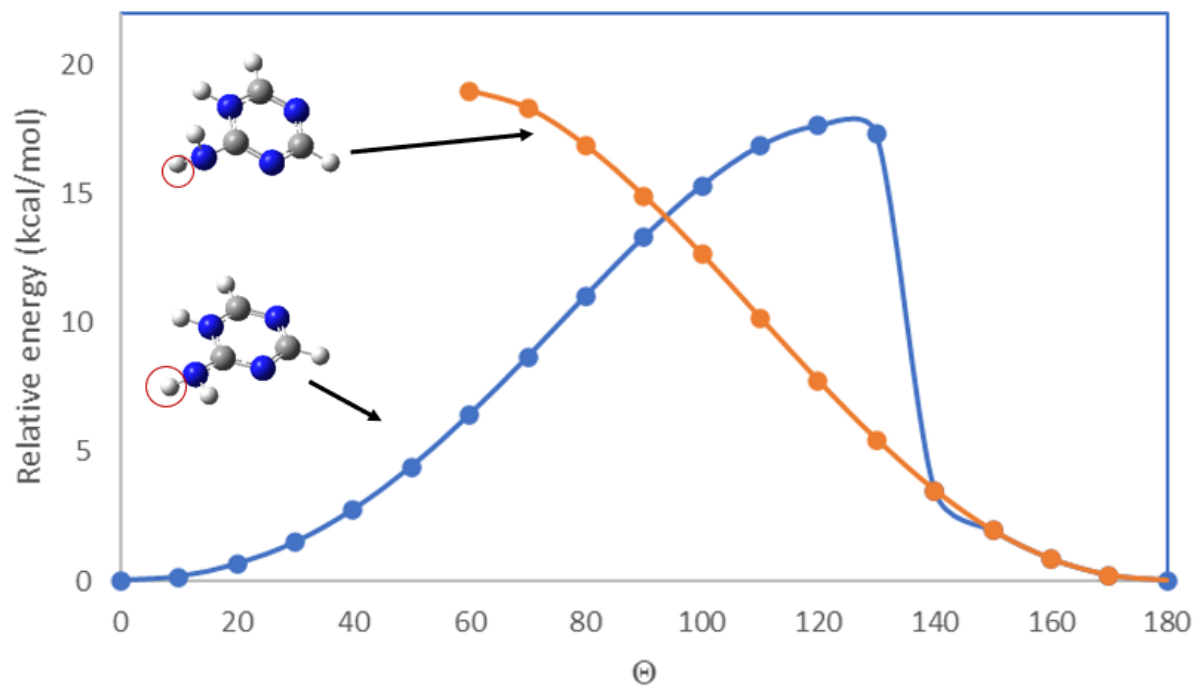


Fig 3.5 Depicts the 1-D potential energy scan of 2-amino-1,3,5-triazine when protonated in the ortho position on the ring nitrogen.

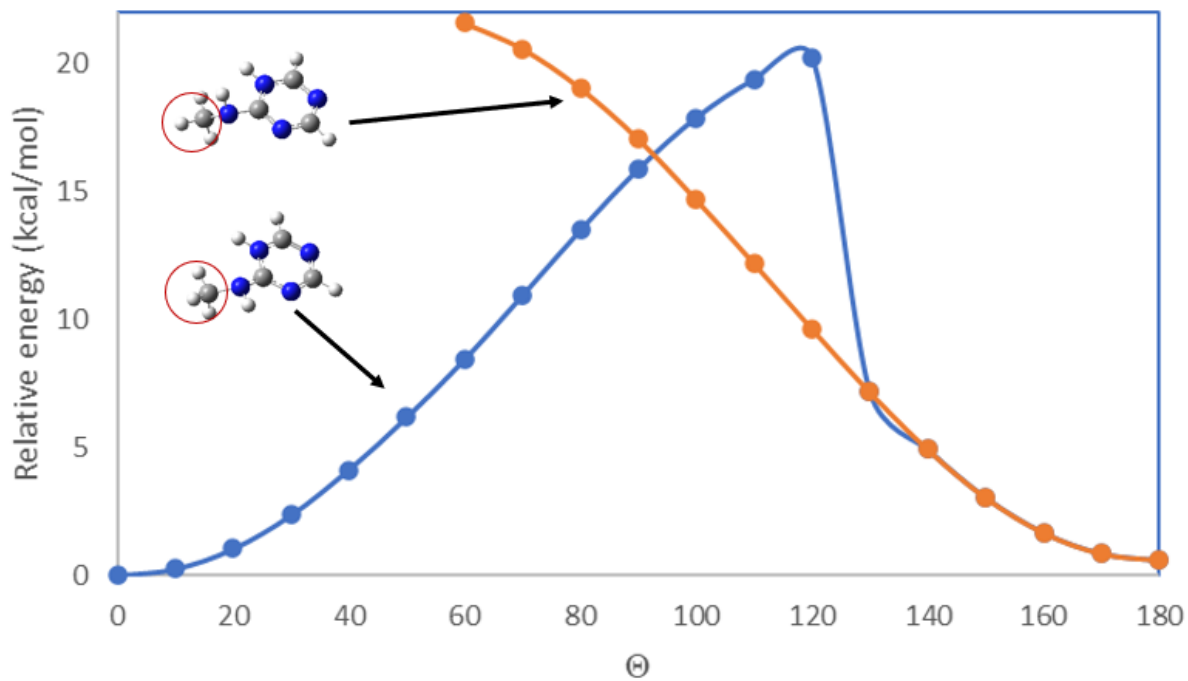


Fig 3.6 Depicts the 1-D potential energy scan of 2-methylamino-1,3,5-triazine when protonated in the ortho position on the ring nitrogen.

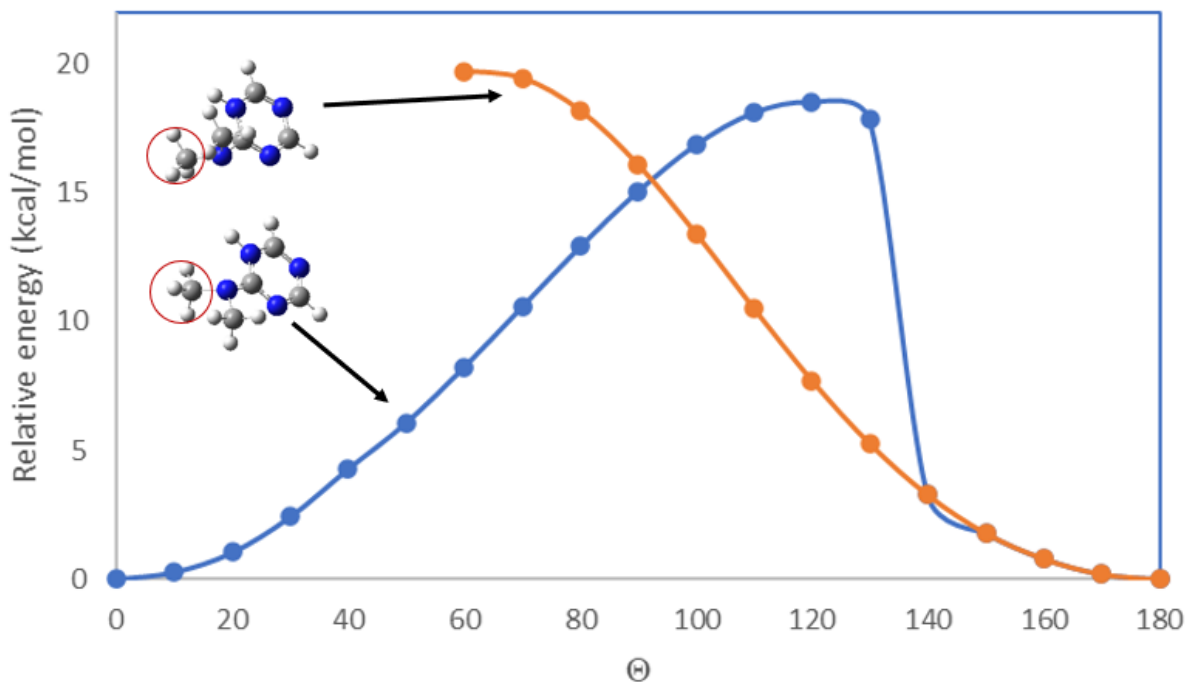


Fig 3.7 Depicts the 1-D potential energy scan of 2-dimethylamino-1,3,5-triazine when protonated in the ortho position on the ring nitrogen.

3.6 *A test of hypothesis 2, that protonation at the NRR' acyclic amino group nitrogen decreases rotational barriers*

Acyclic protonation barriers for 2-amino-1,3,5-triazine, 2-methylamino-1,3,5-triazine, and 2-dimethylamino-1,3,5-triazine are shown in table 3.4. The sp^3 , tetrahedral carbon has a rotational barrier that is several orders of magnitude lower than that of the neutral species. The takeaway, the DFT calculations produce results consistent with the hypothesis that acyclic protonation decreases the rotational barrier of the acyclic amine.

3.7 Acyclic protonation barrier results provide further support that triazines become conformationally flexible at high pH

While the acyclic rotational barriers were initially computed with the intent to prove the concept and to essentially check the work, the PES graphs depict some interesting results that may be experimentally relevant when conditions are acidic enough to protonate on both the ring and amino NRR' site to form a molecule with a 2+ charge.¹⁶ This is relevant to hypothesis 4, which states that triazines become conformationally flexible again at high pH due to acyclic protonation. The rotational barrier depicted in figure 3.8, which is that of 2-amino-1,3,5-triazine, indicates free rotation. While the addition of methyl groups in the case of figure 3.9 (2-methylamino-1,3,5-triazine) and figure 3.10 (2-dimethylamino-1,3,5-triazine) raise the rotational barrier relative to 2-amino-1,3,5-triazine, they still show relatively low energy barriers. This can be attributed to steric interference from the bulkier methyl groups. Figure 3.11 offers a comparative analysis of the rotational barriers of 2-amino-1,3,5-triazine and 2-dimethylamino-1,3,5-triazine. Computed rotational barriers of all three of these species in their doubly protonated, 2+ form (shown in table 3.4) also indicate low rotational barriers of the acyclic amino group. The ultimate takeaway is that these results support the hypothesis that aminotriazines become conformationally flexible at low pH.

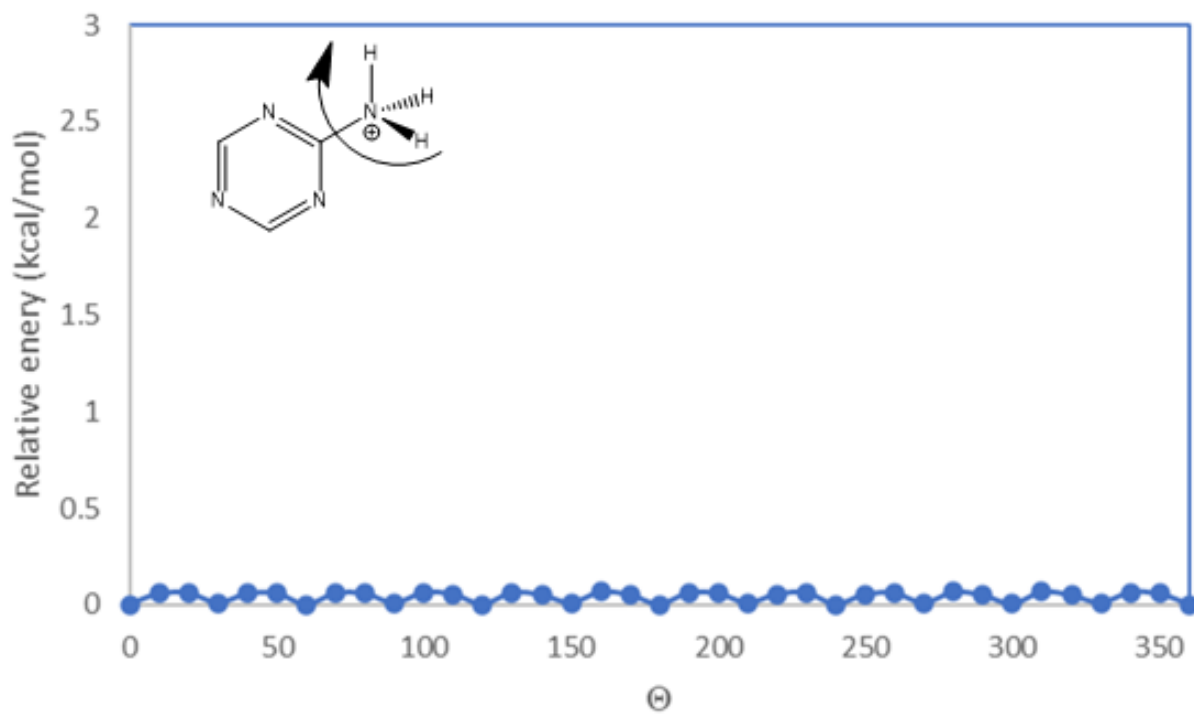


Fig 3.8 Depicts the 1-D potential energy scan of 2-amino-1,3,5-triazine when protonated in the acyclic position.

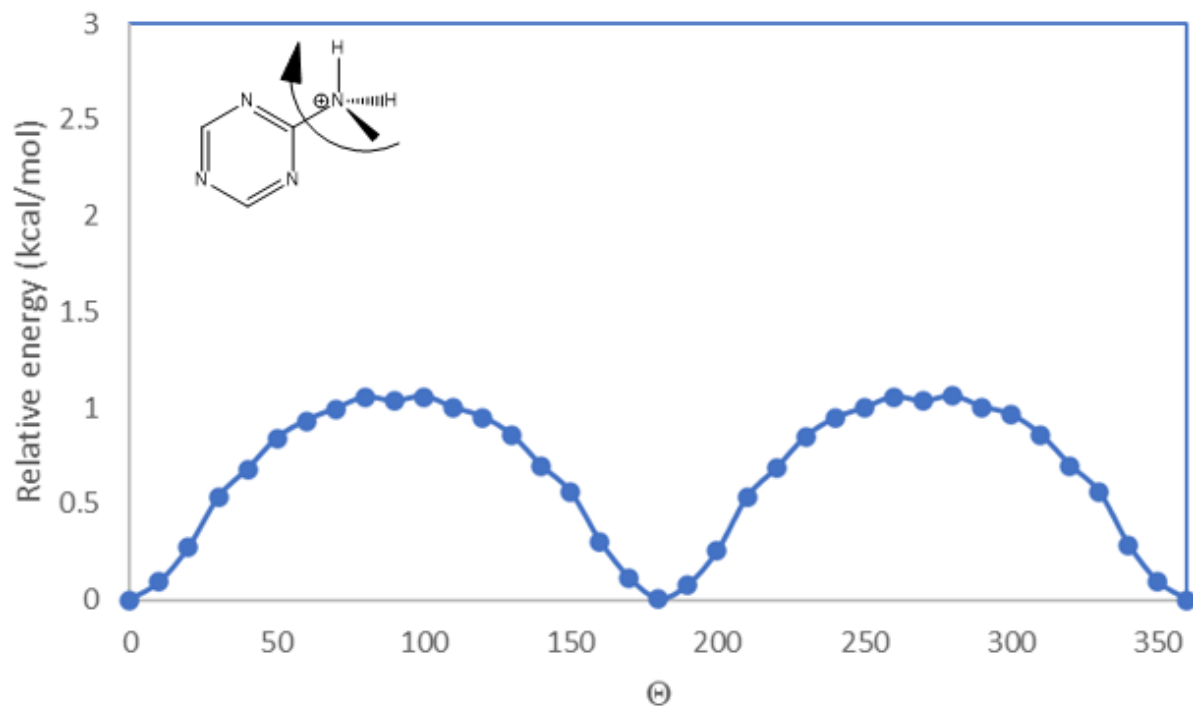


Fig 3.9 Depicts the 1-D potential energy scan of 2-methylamino-1,3,5-triazine when protonated in the acyclic position.

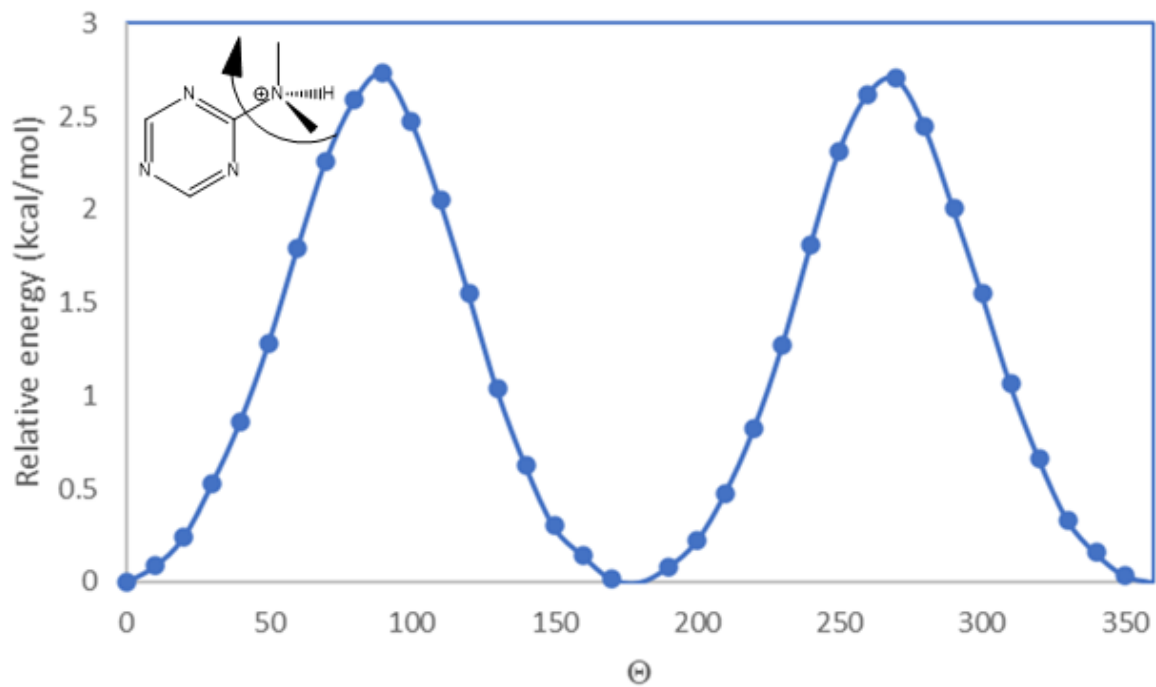


Fig 3.10 Depicts the 1-D potential energy scan of 2-dimethylamino-1,3,5-triazine when protonated in the acyclic position.

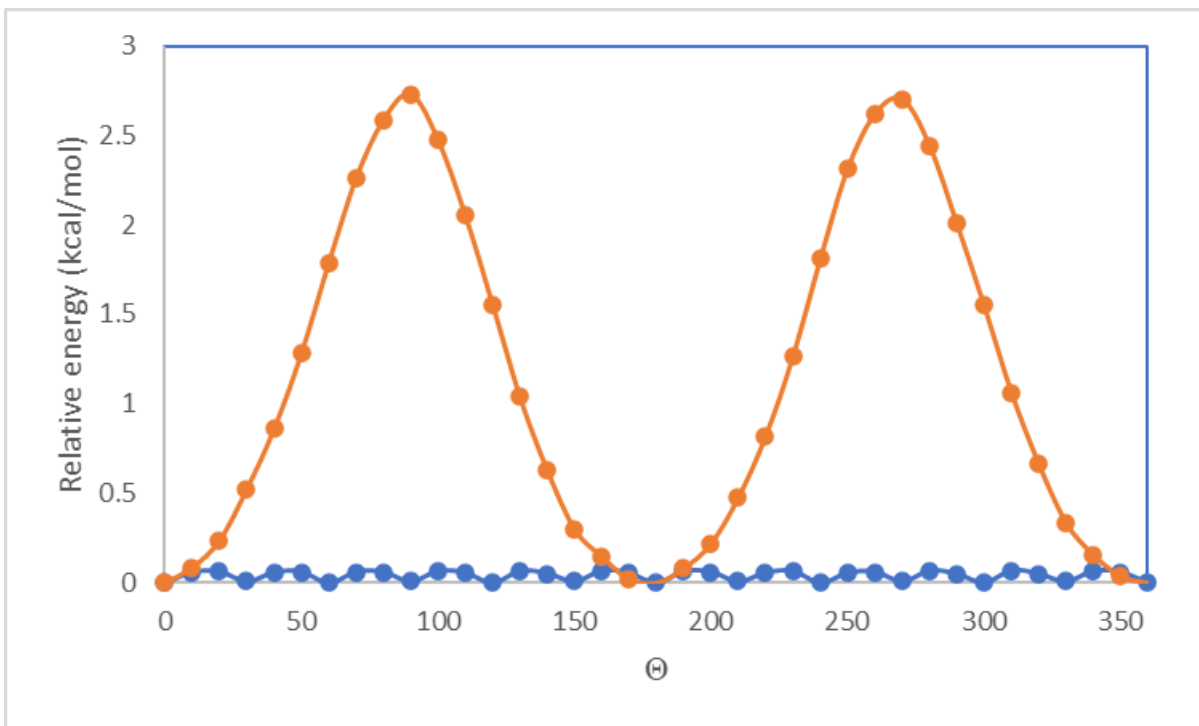


Fig 3.11 The blue curve depicts the 1-D PES of 2-amino-1,3,5-triazine, compared to the 1-D PES of 2-dimethylamino-1,3,5-triazine in orange, one can see just how low the blue curve is when compared to scale with the orange curve.

	2-amino triazine	2-methylamino triazine	2-dimethylamino triazine
Neutral Rotational Barrier (kcal/mol)	11.0	11.7	10.0
Ring Protonation pK_a	-1.04	-0.04	0.25
Ring-Protonated Rotational Barrier (kcal/mol)	13.3	15.9	15.1
Acyclic Protonation pK_a	-9.78	-8.44	-5.96
Acyclic-Protonated Rotational Barrier (kcal/mol)	0.1	1.0	2.8
Doubly protonated pK_a	-24.32	-23.60	-20.76
Doubly Protonated Rotational Barrier (kcal/mol)	0.2	1.3	2.8

Table 3.5 Shows computed rotational barriers and pK_a values for 2-amino-1,3,5-triazine, 2-methylamino-1,3,5-triazine, and 2-dimethylamino-1,3,5-triazine.

4. Discussion

4.1 Rotational barrier discussion

Rotational Barrier calculations by Galvez, et al. test similar aromatic structures. Results from calculations performed on N-methylamino-1,3,5-triazine and 2-aminopyrimidine are most relevant to this study. Calculations using B3LYP/6-311++G(2d,2p) level for each molecule resulted in amino group rotational barriers of 13.65 and 18.09 kcal/mol. The present results are overall consistent given the different levels of theory employed.¹⁵

An important takeaway is that the data is consistent with each hypothesis. Hypothesis 1 is validated because results indicate an increased rotational barrier relevant to the neutral species

when ring protonation occurs in the ortho position. Hypotheses 2 and 4 are validated because rotational barriers of amino groups are lowered relative to the neutral species in acyclic and doubly protonated (+2) species. The tetrahedral sp³ nitrogen produced very low computed energy barriers, and the planar sp² nitrogen produced significantly higher rotational barriers. Hypothesis 3 is validated because computed pK_a values for acyclic species are much lower than the ring protonated species. Overall, calculations produced consistent results and the calculations were consistent with experiment and predictions based on resonance structures.

Practical application of rotational barrier studies relates to experimental work done by Simanek modeling dynamics of triazine based macrocycles and dendrimers in aqueous solution.¹ This computational study relates to experimental work by Simanek that studies rotamer populations of triazines in dendrimers and macrocycles. The main interest is rotamer populations and rotational speed, which our work does an analysis of by modeling rotational barriers.

Work by Simanek on macrocycles investigates triazines with protonation at the ortho position in figure 1.2. In this case, the triazine was like the generic triazines studied here. NMR data indicated that the rotation of the NRR' group was likely slow on an NMR timescale when ortho protonation occurred on the ring nitrogen.² Practically, this means that upon protonation at the ortho position, the rotational barrier will increase relative to the neutral species. Given that the computed rotational barrier increases upon protonation, where neutral species have rotational barriers of 10.98, 11.71, and 9.98 kcal/mol and ortho protonated species have rotational barriers of 13.34, 15.86, and 15.08 kcal/mol respectively, it is fair to conclude that the computational data is consistent with experiment. This validates hypothesis 2 and provides practical application to these computational results.

Regarding triazine dendrimers, it is evident that the conformational isomerism due to rotation of an R group in an acyclic NH(R) group on a triazine on the outermost edge of a dendrimer has a direct effect on population ratios.¹ It appears that the lowest energy structure with the least amount of steric interference has the highest population ratio, which is generally consistent with the exhaustive search performed to find the most stable conformations to calculate the pK_a values, where the least sterically hindered molecule was usually the most energetically favorable.

4.2 pK_a discussion

Using constant entropy resulted in more reasonable results than using non-constant entropy values. This likely indicates that solvent corrections at this level resulted in significant error in the entropy term, further resulting in significant error in the ΔG and pK_a values. pK_a results indicated this may be a useful method for predicting pK_a values for future work. Furthermore, pK_a calculations served a necessary role to validate the hypothesis that ring protonation is preferred over acyclic protonation. This indicates that the DFT methods used are reliable for modeling the dynamics of triazines and melamine derivatives.

5. Conclusion

A detailed proof of concept study was necessary to test the reliability of the methods employed in this study. Had the results not been consistent with our basic knowledge of hybridization and organic chemistry, the method would have proven to be unreliable. Nonetheless, all calculations followed a sensible and predictable trend.

Computations of rotational barriers and pK_a values using the density functional theory (DFT) at the M0-62X/6-311++(2d,2p) level using SMD continuum water produced results consistent with each hypothesis, as well as accurately reproduced experimental results, and in the case of

the rotational barriers, made predictions that were consistent with experimental observations. pH did in fact have a major effect on the conformational dynamics of substituted triazines, evident by the fact that the rotational barrier of an amino NRR' changes drastically upon protonation. The takeaway is that DFT calculations may be used as a powerful tool to predict dynamics of triazines and other similar aromatic ring nitrogen type compounds in solution. This is particularly useful in situations where experimental conditions make an experiment difficult to perform, or when modeling a large system, like a dendrimer or macrocycle may be difficult.

References

1. Moreno, K. X.; and Simanek, E. E. *Macromolecules* **2008**, *41*, 4108-4114.
2. Sharma, V. R.; Mehmood, A.; Janesko, B.G.; Simanek, E.E. *RSC Adv.* **2020**, *10*, 3217.
3. Abbasi, E.; Aval, S.F.; Akbarzadeh, A.; Milani, M.; Nasrabadi, H.T.; Joo, S.W.; Hanifehpour, Y.; Nejati-Koshki, K.; Pashaei-Asl, R.; *Nanoscale Res. Lett.* **2014**, *9*(1), 247.
4. Yudin, A. K.; *Chem. Sci.* **2015**, *6*, 30-49.
5. Simanek, E. E. *Molecules* **2021**, *26*, 4774.
6. Enciso, A.E.; Neun B.; Rodriguez, J.; Ranjan. A. P.; Dobrovolskaia, M. A.; Simanek. E. *Molecules* **2016**, *21*, 428.
7. Solis-Egaña, F.; Lavín-Urqueta, N.; Díaz, D. G.; Mariño-Ocampo, N.; Faúndez, M. A.; Fuentealba, D. *Photochemical & Photobiological Sciences* **2022**
8. Ray, S. S.; Orasugh, J. T. *Polymers* **2022**, *14*, 704.
9. Gaussian 16, Revision C.01, Frisch, M. J.; Trucks, G. W.; Schlegel, H. B.; Scuseria, G. E.; Robb, M. A.; Cheeseman, J. R.; Scalmani, G.; Barone, V.; Petersson, G. A.; Nakatsuji, H.; Li, X.; Caricato, M.; Marenich, A. V.; Bloino, J.; Janesko, B. G.; Gomperts, R.; Mennucci, B.; Hratchian, H. P.; Ortiz, J. V.; Izmaylov, A. F.; Sonnenberg, J. L.; Williams-Young, D.; Ding, F.; Lipparini, F.; Egidi, F.; Goings, J.; Peng, B.; Petrone, A.; Henderson, T.; Ranasinghe, D.; Zakrzewski, V. G.; Gao, J.; Rega, N.; Zheng, G.; Liang, W.; Hada, M.; Ehara, M.; Toyota, K.; Fukuda, R.; Hasegawa, J.; Ishida, M.; Nakajima, T.; Honda, Y.; Kitao, O.; Nakai, H.; Vreven, T.; Throssell, K.; Montgomery, J. A., Jr.; Peralta, J. E.; Ogliaro, F.; Bearpark, M. J.; Heyd, J. J.; Brothers, E. N.; Kudin, K. N.; Staroverov, V. N.; Keith, T. A.; Kobayashi, R.; Normand, J.; Raghavachari, K.; Rendell, A. P.; Burant, J. C.; Iyengar, S. S.; Tomasi, J.; Cossi, M.; Millam, J. M.; Klene, M.; Adamo, C.; Cammi, R.; Ochterski, J. W.; Martin, R. L.; Morokuma, K.; Farkas, O.; Foresman, J. B.; Fox, D. J. Gaussian, Inc., Wallingford CT, 2019.
10. GaussView, Version 6, Dennington, Roy; Keith, Todd A.; Millam, John M. Semichem Inc., Shawnee Mission, KS, 2016.
11. List, M.; Puchinger, H.; Gabriel, H.; Monkowius, U.; Schwarzinger, C. *J. Org. Chem.* **2016**, *81*, 4066–4075.
12. Zhao, Y.; Truhlar, D. G. *Theor. Chem. Acc.*, **2008**, *120*, 215-41.
13. Frisch, M. J.; People, J. A.; J. S. Binkley, J. S. *J. Chem. Phys.*, **1984**, *80*, 3265-69.
14. Marenich, A. V.; Cramer, C. J.; Truhlar, D. G. *J. Phys. Chem. B* **2009**, *113*, 6378-96.
15. Gálvez, J.; López Sánchez, J. I.; Guirado, A. *Computational and Theoretical Chemistry* **2015**, *1069*, 40-47.
16. Jang, Y. H.; Hwang, S.; Chang, S. B.; Ku, J.; Chung, D. S. *J. Phys. Chem. A* **2009**, *113*, 13036–13040.
17. Zeng, Q.; Jones, M. R.; Brooks, B. R. *J. Comput. Aided Mol. Des.* **2018**, *32*(10), 1179–1189.
18. Mech, P.; Bogunia, M.; Nowacki, A.; Makowski, M. *J. Phys. Chem. A* **2020**, *124*, 538–551.
19. Kelly, C. P.; Cramer, C. J.; Truhlar, D. G. *J. Phys. Chem. B* **2006**, *110*, 16066-16081.
20. Atoji, M.; Lipscomb, W. N. *Acta Cryst.* **1953**, *6*, 770.
21. Pearson, Jr., R.; Lovas, F. J. *J. Chem. Phys.* **1977**, *66*, 4149.

22. The author acknowledges the TCU High-Performance Computing Center for providing HPC resources.

VITA

Nicholas Charles Henderson was born December 12, 1996, in the The Woodlands, Texas. He is the son of Charles and Connie Henderson. A 2015 graduate of Mckinney Christian Academy in McKinney, Texas, he received a Bachelor of Science degree with a major in Chemistry and a minor in Mathematics from Texas Christian University in Fort Worth, Texas, in 2019.

Abstract

PH DEPENDENT CONFORMATIONAL DYNAMICS OF SUBSTITUTED TRIAZINES

by Mr. Nicholas Charles Henderson

Department of Chemistry

Texas Christian University

Thesis advisor: Benjamin G. Janesko, Professor of Chemistry

Triazines appear as building blocks for macromolecules used in materials science and medicine. Triazines can be protonated under aqueous conditions, and it is hypothesized that pH changes the conformational dynamics of triazines in solution. Predicting the structure and dynamics in water as a function of pH requires reliable simulations of the rotational barriers and pK_a values for different sites for protonation. We present the initial DFT methods and continuum solvent for pK_a and rotational barriers of amines, ring nitrogens, and 2,4,6-triamino-1,3,5-triazine (melamine) derivatives. These (M062X/6-311++(2d,2p) in SMD continuum water) calculations provide consistent accuracy for tested systems, and results validate the initial hypothesis by showing that rotational barriers of acyclic amino groups change upon ring nitrogen protonation.